ICASE

CR-185787

THE COMPUTATIONAL ACCURACY OF SOME FINITE ELEMENT METHODS FOR

INCOMPRESSIBLE VISCOUS FLOW PROBLEMS

(NASA-CR-185787) THE COMPUTATIONAL ACCURACY OF SOME FINITE ELEMENT METHODS FOR INCOMPRESSIBLE VISCOUS FLOW PROBLEMS (ICASE) 21 p

N89-71408

Unclas

00/34 0224384

Max D. Gunzburger

and

R. A. Nicolaides

Report No. 81-7

February 3, 1981

INSTITUTE FOR COMPUTER APPLICATIONS IN SCIENCE AND ENGINEERING

NASA Langley Research Center, Hampton, Virginia

Operated by the

UNIVERSITIES SPACE USRA RESEARCH ASSOCIATION

THE COMPUTATIONAL ACCURACY OF SOME FINITE ELEMENT METHODS FOR INCOMPRESSIBLE VISCOUS FLOW PROBLEMS

Max D. Gunzburger
University of Tenneessee, Knoxville

and

R. A. Nicolaides
Carnegie-Mellon University

ABSTRACT

The asymptotic rates of convergence for the approximate solution of the stationary Stokes equations is numerically determined for some particular choices of conforming finite element spaces. These rates are for norms which are of physical interest. It is shown that some simple finite elements introduced here are at least as accurate as a considerably more complicated element which is popular in the literature.

This work was partially supported by the Air Force Office of Scientific Research under Grants No. AF-AFOSR-80-0083 and AF-AFOSR-80-0091, and in part by NASA Contract No. NAS1-15810 while the authors were in residence at the Institute for Computer Applications in Science and Engineering (ICASE), NASA Langley Research Center, Hampton, VA 23665.

1. Introduction

This paper is concerned with the conforming finite element solution of the stationary Stokes equations of incompressible viscous flow. Although we do not attempt to solve the full nonlinear Navier-Stokes equations, it seems reasonable that the results presented have definite relevance to that case. Mainly, we present the results of numerical calculations designed to evaluate the accuracy of some particular finite elements, both old and new. Although the existing literature contains a fair amount of reporting of numerical results, most of it does not aim at assessing the asymptotic convergence rates. Rather, authors tend to assess the suitability of the approximations on the basis of some empirical criterion, such as a visual presentation of the flow field. Here, we attempt to assess the asymptotic rates of convergence of approximations to smooth solutions of the equations in the norms of $\vec{H}_0^1$ and $\vec{L}^2$ for the velocity field, and L^2 for the pressure field. The two norms on the velocity errors are both of physical interest, e.g. in the computation of shear stresses in the first case, and the construction of flow fields in the second. As is usual with the asymptotic type of analysis, interest is directed to those finite elements which achieve approximation theoretical accuracy to the true solutions in the norms of interest.

Section 2 contains an outline of the theory of the error estimates at a level of detail sufficient for understanding the remainder of the paper. In section 3 we introduce the finite elements which will be used to generate the approximations, and in section 4 we present the numerical results along with our conclusions.

2. Error Theory

The equations to be solved are the following:

$$a(\underline{u},\underline{v}) + b(p,\underline{v}) = \langle \underline{f},\underline{v} \rangle \ , \tag{2.1}$$

$$b(q,\underline{u}) = [g,q] \ , \tag{2.2}$$

where

$$a(\underline{u},\underline{v}) = \int_\Omega \nabla\underline{u} : \nabla\underline{v} \qquad \forall \quad \underline{u},\underline{v} \in \vec{H}_0^1(\Omega), \tag{2.3}$$

$$b(q,\underline{v}) = \int_\Omega q \operatorname{div} \underline{v} \qquad \forall \quad q \in \bar{L}^2(\Omega) \qquad \underline{v} \in \vec{H}_0^1(\Omega) \ . \tag{2.4}$$

$\vec{H}_0^1(\Omega)$ denotes the Hilbert space of real valued 2 or 3 dimensional velocity fields whose components have a distributional derivative in $L^2(\Omega)$ in each variable and which have zero trace on $\partial\Omega$, normed by

$$\|\underline{v}\|^2_{\vec{H}_0^1(\Omega)} = \int_\Omega \nabla\underline{v} : \nabla\underline{v} \ . \tag{2.5}$$

In (2.3) - (2.5) the colon denotes the sum of the products of the components of the tensor standing on each side of it. In (2.4) $\bar{L}^2(\Omega)$ denotes the linear subspace of $L^2(\Omega)$ of elements orthogonal to constants. Ω is a domain in R^2 or R^3 where the velocity and pressure distributions are sought.

In (2.1) - (2-2), $\underline{f}$ and g denote bounded linear functionals respectively on $\vec{H}_0^1(\Omega)$ and $\bar{L}^2(\Omega)$. The viscosity parameter ν has been absorbed into the pressure field p, and also affects the scaling of $\underline{f}$ and g.

The finite element scheme used is the standard one, namely $V^h \subset \vec{H}_0^1(\Omega)$ and $S^h \subset \bar{L}^2(\Omega)$ are chosen and approximations $\underline{u}^h, p^h$ are defined by

$$(2.6) \qquad a(\underline{u}^h,\underline{v}^h) + b(p^h,\underline{v}^h) = \langle \underline{f},\underline{v}^h\rangle \qquad \forall \quad \underline{v}^h \in \mathcal{V}^h,$$

$$(2.7) \qquad b(q^h,\underline{u}^h) = [g,q^h] \qquad \forall \quad q^h \in \mathcal{S}^h.$$

In order to describe the error analysis, some notation is required. Let $\mathcal{Z} \in \vec{H}_0^1(\Omega)$ and $\mathcal{Z}^h \in \mathcal{V}^h$ be defined as follows:

$$(2.8) \qquad \mathcal{Z} = \{\underline{z} \subset \vec{H}_0^1(\Omega) \mid b(q,\underline{z}) = 0 \quad \forall \quad q \subset \bar{L}^2(\Omega)\},$$

$$(2.8') \qquad \mathcal{Z}^h = \{\underline{z}^h \subset \mathcal{V}^h \mid b(q^h,\underline{z}^h) = 0 \quad \forall \quad q^h \subset \mathcal{S}^h\}.$$

Roughly speaking, $\mathcal{Z}$ is the subspace of $\vec{H}_0^1(\Omega)$ of solenoidal fields and $\mathcal{Z}^h$ is the subspace of $\mathcal{V}^h$ of "discretely solenoidal" fields. It is necessary to realize that in general, $\mathcal{Z}^h \not\subset \mathcal{Z}$.

Analysis of the error between the solutions of (2.1) - (2.2) and (2.6) - (2.7) was given in [1], generalizing previous work, particularly [2]. The analysis was based on the application of the Babuška theory to the equation on $\vec{H}_0^1 \times \bar{L}^2$

$$B[(\underline{u},p),(\underline{v},g)] = \{(\underline{f},g),(\underline{v},q)\},$$

representing (2.6) - (2.7), in the obvious way. The resulting error estimate, obtained in the graph norm

$$|||(\underline{v},q)|||_{\vec{H}_0^1 \times \bar{L}^2} \equiv \|\underline{v}\|_{\vec{H}_0^1(\Omega)} + \|q\|_{\bar{L}^2(\Omega)},$$

gives the usual result

$$(2.9) \qquad |||(\underline{u}-\underline{u}^h,p-p^h)||| < C\left\{\inf_{(\hat{u}^h,\hat{p}^h) \in \mathcal{V}^h \times \mathcal{S}^h} \left(|||(\underline{u}-\hat{\underline{u}}^h,p-\hat{p}^h)|||\right)\right\}.$$

Often, one is interested in the errors $\|\underline{u}-\underline{u}^h\|_{\vec{H}_0^1(\Omega)}$ and $\|p-p^h\|_{L^2(\Omega)}$.

Clearly, for the first of these, (2.9) gives

$$(2.10)\qquad \|\underline{u}-\underline{u}^h\|_{\vec{H}_0^1} \le C\left\{\inf_{\hat{\underline{u}}^h\in \mathcal{V}^h}\|\underline{u}-\hat{\underline{u}}^h\|_{\vec{H}_0^1} + \inf_{\hat{p}^h\in \mathcal{S}^h}\|p-\hat{p}^h\|_{\bar{L}^2}\right\},$$

with a similar estimate for $\|p-p^h\|_{\bar{L}^2}$. However, these are not the most precise estimates obtainable, even without changing the hypotheses. The more precise estimates, given in [6], are

$$(2.11)\qquad \|\underline{u}-\underline{u}^h\|_{\vec{H}_0^1} \le C_1 \inf_{\hat{\underline{u}}^h\in \mathcal{V}^h}\|\underline{u}-\hat{\underline{u}}^h\|_{\vec{H}_0^1} + C_2\Gamma(Z,Z^h)\inf_{\hat{p}^h\in \mathcal{S}^h}\|p-\hat{p}^h\|_{L^2},$$

$$(2.12)\qquad \|p-p^h\|_{L^2} \le C_1' \inf_{\underline{u}^h\in \mathcal{V}^h}\|\underline{u}-\hat{\underline{u}}^h\|_{\vec{H}_0^1} + C_2' \inf_{p^h\in \mathcal{S}^h}\|p-\hat{p}^h\|_{L^2}.$$

(2.12) is sufficiently similar to the corresponding estimate obtained from the graph norm to require no discussion except to point out the improvement in the distribution of the constants. (2.11) though, contains new information in the multiplier $\Gamma(Z,Z^h)$ defined by

$$(2.13)\qquad \Gamma(Z,Z^h) = \sup_{\substack{\underline{z}^h\in Z^h\\ \|\underline{z}^h\|=1}} \inf_{\underline{z}\in Z}\|\underline{z}-\underline{z}^h\|_{\vec{H}_0^1}.$$

For example, if $Z^h \subset Z$, then $\Gamma(Z,Z^h) = 0$. Generally, $\Gamma(Z,Z^h)$ is a measure of the angle between the linear manifolds Z and $Z^h \subset \vec{H}_0^1(\Omega)$. If $\Gamma(Z,Z^h) = 0$, then (2.11) shows that the error in the velocity field is completely independent of the error in the pressure field. However, (2.10) does not predict this independence. Thus (2.11) contains more information than (2.10). Although it has not been proved, it seems reasonable that (2.11) is a sharp estimate in all cases, and not only when $\Gamma(Z,Z^h) = 0$. For these reasons, we will regard (2.11) - (2.12) as our error estimates for the velocity error in $\vec{H}_0^1(\Omega)$ and the pressure error in $L^2(\Omega)$. In later sections, examples of the application of these estimates will be given.

One further point concerns the errors $\| \underline{u} - \underline{u}^h \|_{\vec{L}^2(\Omega)}$, this being the sum of the squares of the $L^2(\Omega)$ norms of the components of the error. To obtain this error from (2.11) - (2.12) is a straight forward application of the standard duality argument, provided $\underline{u}$ is sufficiently smooth, and yields the expected result that

$$\| \underline{u} - \underline{u}^h \|_{\vec{L}^2} \leq Ch \| \underline{u} - \underline{u}^h \|_{\vec{H}_0^1}, \tag{2.14}$$

where h has the usual significance of a measure of the grid size.

3. Finite Elements

A basic fact about non-positive definite problems such as (2.1) - (2.2) is that in general, discrete approximation procedures are unstable. (This can be anticipated for the symmetric cases - like (2.1) - (2.2) - from theorems about eigenvalues of constrained operators interlacing those of corresponding but less constrained operators.) Thus, it is necessary to exercise care in the choice of approximation spaces $\mathcal{V}^h$ and $\mathcal{S}^h$. There are several conditions that must hold for stability to be guaranteed, and they may be found, e.g. in [1] or [6]. The most important one, in the sense of it being the one which fails to be satisfied in the unstable cases will now be introduced. Let $\mathcal{W}^h$ denote the orthogonal complement of $\mathcal{Z}^h$ in $\mathcal{V}^h$, so that

$$\mathcal{V}^h = \mathcal{Z}^h \oplus \mathcal{W}^h. \tag{3.1}$$

Let $\mathrm{div}_h : \mathcal{V}^h \to \mathcal{S}^h$ be defined by the relation

$$b(q^h, \underline{v}^h) \equiv \int_\Omega q^h \mathrm{div}_h \underline{v}^h \qquad \forall \quad q^h \in \mathcal{S}^h, \tag{3.2}$$

where $b(\cdot,\cdot)$ is defined by (2.4). The necessary stability condition is the following:

$$\|\operatorname{div}_h \underline{w}^h\|_{L^2} \geq \gamma^2 \|\underline{w}^h\|_{\vec{H}_0^1} \qquad \gamma^2 > 0, \tag{3.3}$$

where $\gamma^2 \neq \gamma^2(h)$. We mention that the conditions necessary for the existence of the decomposition (3.1) and the operator div_h will always hold for the problem set up as described in section 2. See e.g. [1], [6] for these details. (3.3) is not easy to prove in general, and we will not attempt to provide proofs for the elements discussed below. However, it should be pointed out that (3.3) has in fact been proved for each of these cases [3]. In choosing $\mathcal{V}^h$ and $\mathcal{S}^h$, some decision must be made about the degrees of the element polynomials in each case. In fact, before this can be done a triangulation must be established for $\mathcal{V}^h$, and another one for $\mathcal{S}^h$. Although in the literature these triangulations are usually taken as coincident there is no <u>a priori</u> reason for it, and some of the elements below use different - although not unrelated - triangulations.

(2.11) shows that if the mesh sizes of $\mathcal{V}^h$ and $\mathcal{S}^h$ are comparable, then, since $0 \leq \Gamma(Z,Z^h) \leq 1$, the degree of $\mathcal{S}^h$ should be one less than that of $\mathcal{V}^h$. We refer to this as "comparability". In this case, the two error terms are of the same order in h. However, this condition is not necessary for $\vec{H}_0^1$ convergence, although it probably is necessary for optimal $\vec{H}_0^1$ convergence. It is assumed of course that the chosen elements form a stable combination in the sense of (3.3).

As an example of an unstable discretization, it is necessary to look no further than the triangulation of a square by the method shown in Figure 1. Defining $\mathcal{V}^h$ to be all piecewise linear fields, vanishing on the boundary and $\mathcal{S}^h$ to be all piecewise constants on the triangles with mean zero over

the square, it may be simply shown from (3.2) that

$$\operatorname{div}_h \underline{v}^h \equiv \operatorname{div} \underline{v}^h \qquad \forall \quad v^h \in \mathcal{V}^h.$$

On the other hand, inspection of Fig. 1 and use of the boundary conditions on $\underline{v}^h$ and the definition of $\operatorname{div} \underline{v}^h$ shows that

$$\operatorname{div} \underline{v}^h = 0 \quad \text{implies} \quad \underline{v}^h = 0.$$

But then $Z^h = 0$, so $\mathcal{W}^h \equiv \mathcal{V}^h$ and therefore, (3.3) must hold for every $\underline{v}^h \in \mathcal{V}^h$. But clearly, by choosing $\underline{v}^h$ such that $\| v^h \|_{\vec{H}^1_0} = 1$ and $\underline{v}^h$ is a best $\vec{H}^1_0(\Omega)$ approximation to a solenoidal field, we can make $\| \operatorname{div}_h \underline{v}^h \|_{\vec{H}^1_0} \to 0$ so (3.3) cannot hold and the scheme is unstable in this sense.

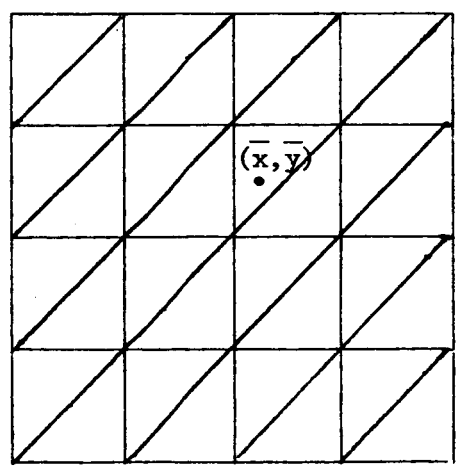

$(\bar{x},\bar{y})$ is the centroid of a triangle.

Figure 1.

A stable scheme, apparently first suggested in [2], is obtained by using the same S^h as before and taking for $\mathcal{V}^h$ all continuous piecewise quadratic fields vanishing on $\partial\Omega$. This scheme, for which computational

results are reported below violates the requirement for optimal $\vec{H}_0^1(\Omega)$ accuracy in the computed velocity (but not for optimality in the graph norm); it follows from (2.11) that the vector error is dominated by the last term (it can be shown that $\Gamma(Z,Z^h) = 1$ for this element pair).

Another technique for stabilizing the unstable scheme mentioned above is as follows [8]; first we discuss this for the square of Figure 1

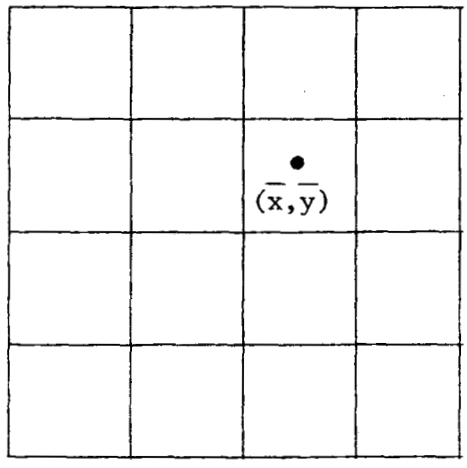

$(\bar{x},\bar{y})$ is the centroid of the box shown.

Figure 2

and Figure 2. This time, V^h does not change, but S^h is defined as all piecewise constants with mean over Ω equal to zero, defined on the triangulation of Figure 2. This is an example of distinct, although closely related triangulations being used for V^h and S^h. The comparability condition for optimal $\vec{H}_0^1(\Omega)$ accuracy is evidently satisfied, and it is possible to show the stability of the combination. In general, the region would be divided into quadrilaterals, in each of which a constant pressure distribution is assumed, and a continuous piecewise linear velocity field defined by splitting each quadrilateral into 2 triangles by drawing a diagonal. This element combination is stable and computational results for it are reported below.

Our third scheme has the distinguishing feature that for it, div_h coincides with div, (so that $\Gamma(Z,Z^h) = 0$). Also, the scheme is stable. This scheme makes use, for the square region, the triangulation shown in Figure 3.

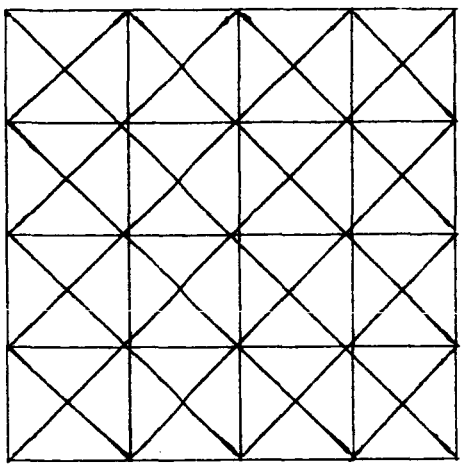

Figure 3

Once again, V^h is taken as the class of all continuous piecewise linear fields, zero on $\partial\Omega$. S^h is a certain subspace of the class of all piecewise constants on the triangles of the subdivision. This class is in fact defined as $S^h \equiv \mathrm{div}\ V^h$. A convenient basis for the space is, referring to Figure 4, defined within each box ABCD, by the characteristic functions of the triangles ABD, ABC, and BCD. The basis is three dimensional within each box, rather than four dimensional, because there is a constraint forced on the four constants by the divergence theorem. See [4] for more details of this element pair.

The fourth and final scheme, unlike the three previous ones is restricted to regions whose boundaries are straight lines parallel to the coordinate axes, since it uses bilinear elements for V^h and, once again piecewise

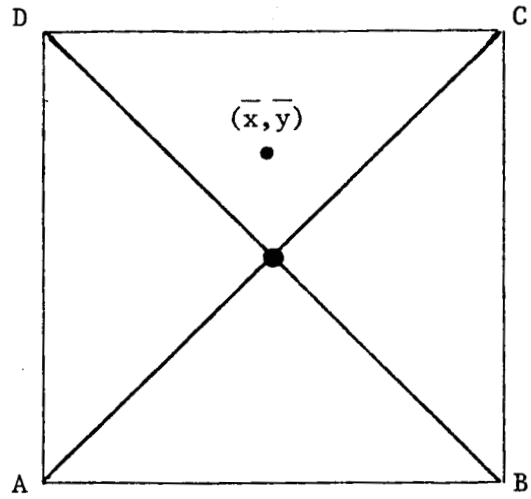

$(\bar{x},\bar{y})$ is the centroid of a triangle.

Figure 4.

constant elements with mean zero for the pressure field. The triangulation of Figure 2 would be appropriate for this pair of elements. Again the comparability condition holds, and optimal $\vec{H}_0^1$ accuracy should be obtained.

4. Computational Results and Discussion

In order to compute the asymptotic error behavior as a function of h, (2.1) - (2.2) was solved in the region

$$\Omega = \{(x,y) \mid 0 < x,\ y < 1\},$$

for a problem whose exact solution is

$$\underline{u} = \begin{Bmatrix} \sin \pi x \sin 2\pi y \\ x^2(1-x)\sin \pi y \end{Bmatrix}$$

$$p = (1 - 4y + y^3)\cos \pi x \ .$$

For this choice of $\underline{u}$ and p, both $\underline{f}$ and g in (2.1) - (2.2) will be nonzero, although $u|_{\partial\Omega} = 0$. Generally in incompressible flow $g = 0$, but the fact that here it is $\neq 0$ does not affect the validity of the results below when $g = 0$. This is because for smooth solutions the <u>rates</u> of convergence in the estimates (2.11) - (2.12), and (2.14) are independent of $\underline{f}$ and g. For instance, in (2.11), using linear velocity and constant pressure elements we obtain

$$\| \underline{u} - \underline{u}^h \|_{\vec{H}_0^1} \leq h(C_1 \| \underline{u} \|_2 + C_2 \| p \|_1),$$

and only the <u>multiplier</u> of h depends on $\underline{f}$ and g.

For brevity, the four pairs of trial functions will be called P1(Quadratic/constant), P2(Linear/constant on boxes), P3(linear/constant as in Figs. 3 and 4), P4(Bilinear/constant). They are described in this order in section 3. The triangulation used was in each case the regular one defined in the appropriate paragraph of section 3.

For the computations themselves, the problem was solved in each case using a sequence of grid sizes $h = 1/7$ to $h = 1/14$. The discrete linear systems were solved in each case by a banded elimination solver with partial pivoting; this is necessary since the assembled coefficient matrix, while symmetric, is indefinite. Regarding the imposition of the pressure normalization condition

$$\int_\Omega p^h = 0, \tag{4.1}$$

it was found most simple to assign an arbitrary variable at the end of the forward sweep. The resulting solution must, of course, now be projected orthogonally to the constant pressure field to obtain a solution satisfying (4.1).

For elements P2 - P4, it turns out that a further (not "physical") orthogonality condition has to be imposed on p^h in order to obtain a unique solution to the equations. Rather than discuss a detailed approach (actually another projection) we merely observe that no matter what orthogonalities are required of the pressure, once the velocity field $\underline{u}^h$ is found, the pressure can always be computed - at some cost - as the least squares solution to the algebraic equivalent of the first differential equation (2.1). This computation will not be discussed any further here as our aim is to assess convergence rates, rather than to discuss solution algorithms; the latter is a large enough subject in its own right, and will be discussed in detail elsewhere [7].

Instead of computing the error $\underline{u} - \underline{u}^h$, we actually computed $I_h\underline{u} - \underline{u}^h$, where I_h is the pointwise interpolation operator from $\underline{u} \to \underline{\tilde{u}}^h = I_h u \in V^h$. The following norms were computed

$$\| I_h\underline{u} - \underline{u}^h \|_{\underline{H}_0^1} , \tag{4.2}$$

$$\| I_h\underline{u} - \underline{u}^h \|_{\underline{L}^2} . \tag{4.3}$$

By the triangle inequality

$$\| \underline{u} - \underline{u}^h \|_* \leq \| \underline{u} - I_h\underline{u} \|_* + \| I_h\underline{u} - \underline{u}^h \|_* , \tag{4.4}$$

where $\| \cdot \|_*$ denotes either of the norms in (4.2) - (4.3). Since the first term on the right of (4.4) is purely approximation theoretical it can be easily estimated for smooth solutions. Therefore an estimate for the left hand side can be obtained from estimates of the second term on the right.

Concerning the pressure field errors, the same method was used. In order to give a complete description however we have to specify the particular points at which the pressure interpolant was formed. These are as follows:

$$\begin{aligned} P1 &: \tilde{I}_h p = p(\bar{x},\bar{y}), && [\text{Fig. } 1] \\ P2,\ P4 &: \tilde{I}_h p = p(\bar{x},\bar{y}), && [\text{Fig. } 2] \\ P3 &: \tilde{I}_h p = p(\bar{x},\bar{y}). && [\text{Fig. } 4] \end{aligned}$$

Tables 1-4 contain the computed convergence rates for the $L^2(\Omega)$ error in the pressure and the $\vec{L}^2(\Omega)$ and $\vec{H}_0^1(\Omega)$ errors for the velocities for each of the element pairs P1 - P4. These, as discussed above, are then relative to the interpolants. The rates themselves are computed by assuming that the errors in every case have the form Ch^α, and then computing α between each pair of successive grids by the formula

$$\alpha = \ln\left(\frac{\varepsilon_2}{\varepsilon_1}\right) / \ln\left(\frac{h_2}{h_1}\right) ,$$

where ε_i denote any of the errors.

For P2 - P4 the rates given in the tables are at least as great as the corresponding rates for the approximation error and therefore by (4.4) the rate of convergence of the error will be no worse than that given by the approximation theoretic part. In these three cases,

$$\begin{aligned} &\| p - p^h \|_{L^2} = O(h) \\ (4.5) \qquad &\| \underline{u} - \underline{u}^h \|_{\vec{L}^2} = O(h^2) \\ &\| \underline{u} - \underline{u}^h \|_{\vec{H}_0^1} = O(h) . \end{aligned}$$

The rates given in Table 1 on the other hand show that in (4.4) the velocity errors are dominated by the second term on the right hand side. For example, the $\vec{H}_0^1$ approximation error is $O(h^2)$ while by Table 1, the second term in (4.4) is at best $O(h)$. Strictly speaking, this does not imply that $\| \underline{u} - \underline{u}^h \|_{\vec{H}_0^1}$ is not $O(h^2)$; however, direct computation of this error based on use of a high order quadrature formula show that the error is at best $O(h)$. In fact, the estimates (4.5) hold for P1, in spite of the fact that it is considerably more complex to compute with than the other element pairs.

We note that in some instances the rates measured relative to the interpolant are one order higher than the corresponding rates for the approximation error. This happens for the pressures for P1, P2 and P4 (see Tables 1, 2, and 4). Although Table 3 does not show such behavior for P3, by averaging the numerical solution in each box and measuring relative to the true solution at the box center, the same improvement in the rate is obtained. For the $\vec{H}_0^1$ error in the vector field, only P2 and P4 show this improvement. This form of "superconvergence" is potentially useful for example, when linear functionals of the true solution are to be approximated.

Finally, it is clear that it would be desirable to have element pairs, achieving arbitrary accuracy as in the positive definite case. See [5] in this connection.

REFERENCES

[1] F. Brezzi, *On the existence uniqueness and approximation of saddle point problems arising from Lagrangian multipliers*, R.A.I.R.O., 8-R2, (1974), pp. 129-151.

[2] M. Crouzeix and P. A. Raviart, *Conforming and nonconforming finite element methods for solving the stationary Stokes equations*, R.A.I.R.O., 7-R2, (1973), pp. 33-76.

[3] G. Fix, *A general theory of mixed finite element methods*, (to appear).

[4] G. Fix, M. Gunzburger, and R. Nicolaides, *On mixed finite element methods for first order elliptic systems*, (to appear in Numer. Math.).

[5] L. Mansfield, *Finite element subspaces with optimal rates of convergence for the stationary Stokes problem*, (to appear).

[6] R. Nicolaides, *Existence, uniqueness and approximation for generalized saddle point problems*, (to appear SIAM J. Numer. Anal.).

[7] R. Nicolaides, *Solution of discretized Stokes and related equation systems*, (to appear).

[8] R. Nicolaides, *Co-energy methods for elliptic flow and related problems*, Proc. of Elliptic Problem Solvers Conference, Los Alamos Scientific Laboratory, Santa Fe, NM, June 30-July 2, 1980.

TABLE 1

Rates of convergence for element pair P1

h	$\alpha(\lVert \tilde{p}^h - p^h \rVert_{L^2})$	$\alpha(\lVert \tilde{\underline{u}}^h - \underline{u}^h \rVert_{\vec{L}^2})$	$\alpha(\lVert \tilde{\underline{u}}^h - \underline{u}^h \rVert_{\vec{H}_0^1})$
1/7			
	1.638	1.906	1.029
1/8			
	1.658	1.904	1.002
1/9			
	1.674	1.906	.987
1/10			
	1.689	1.909	.978
1/11			
	1.703	1.913	.973
1/12			
	1.715	1.917	.970
1/13			
	1.725	1.921	.969
1/14			

TABLE 2

Rates of convergence for element pair P2

h	$\alpha(\|\tilde{p}^h - p^h\|_{L^2})$	$\alpha(\|\tilde{\underline{u}}^h - \underline{u}^h\|_{\vec{L}^2})$	$\alpha(\|\tilde{\underline{u}}^h - \underline{u}^h\|_{\vec{H}_0^1}$
1/7			
	2.151	2.022	2.084
1/8			
	2.250	2.015	2.065
1/9			
	2.098	2.003	2.047
1/10			
	2.149	2.011	2.044
1/11			
	2.045	1.990	2.021
1/12			
	2.124	2.017	2.041
1/13			
	2.007	2.001	2.024
1/14			

TABLE 3

Rates of convergence for element pair P3

h	$\alpha(\|\tilde{p}^h - p^h\|_{L^2})$	$\alpha(\|\tilde{\underline{u}}^h - \underline{u}^h\|_{\vec{L}^2})$	$\alpha(\|\tilde{\underline{u}}^h - \underline{u}^h\|_{\vec{H}_0^1})$
1/7			
	1.269	2.129	1.028
1/8			
	1.219	2.114	1.020
1/9			
	1.153	2.087	1.013
1/10			
	1.139	2.066	1.012
1/11			
	1.099	2.062	1.008
1/12			
	1.096	2.043	1.008
1/13			
	1.069	2.042	1.006
1/14			

TABLE 4

Rates of convergence for element pair P4

h	$\alpha(\|\tilde{p}^h - p^h\|_{L^2})$	$\alpha(\|\tilde{\underline{u}}^h - \underline{u}^h\|_{\vec{L}^2})$	$\alpha(\|\tilde{\underline{u}}^h - \underline{u}^h\|_{\vec{H}_0^1})$
1/7			
	2.130	2.007	2.053
1/8			
	2.275	1.968	2.004
1/9			
	1.925	1.967	1.995
1/10			
	2.339	2.017	2.042
1/11			
	1.899	1.999	2.017
1/12			
	2.282	1.986	2.005
1/13			
	1.833	1.998	2.012
1/14			